Thermal and Dielectric Performance of Ester Oil-Based Pentyl-Graphene Nanofluids

Manal M. Emara, *Member, IEEE*, Georgios D. Peppas, *Member, IEEE*, Eleftheria C. Pyrgioti, *Member, IEEE*, Demetrios D. Chronopoulos, Aristides Bakandritsos, Sokratis N. Tegopoulos, Apostolos Kyritsis, Thomas E. Tsovilis, *Senior Member, IEEE*, Aikaterini D. Polykrati, and Ioannis F. Gonos, *Senior Member, IEEE*

***Abstract*— This work reports on the significant enhancement of the thermal properties of the FR3 natural ester dielectric oil after the addition of pentyl-graphene nanosheets, as confirmed by thermal diffusivity and specific heat studies at different concentrations and temperatures (30 °C–90 °C). Experimental results of the dielectric constant demonstrated a constant value in the kHz region while increased in the low-frequency region, decreased with increased temperature, and saturated at 0.008% w/w concentration. In addition, light absorption is used for a better understanding of the properties variation upon changing graphene's concentration as a method to estimate the agglomeration level. The optimum concentration for its best performance in terms of thermal and dielectric properties is 0.008% w/w, whereby the thermal diffusivity and the dielectric constant increased by 43.04% and 6.18%, respectively.**

***Index Terms*— Dielectric properties, electrical conductivity, nanofluids, nanoparticles, permittivity measurements, thermal conductivity.**

Manuscript received April 12, 2021; accepted March 3, 2022. Date of publication March 31, 2022; date of current version May 2, 2022. *(Corresponding author: Manal M. Emara.)*

Manal M. Emara was with the School of Electrical and Computer Engineering, National Technical University of Athens, 15780 Athens, Greece. She is now with the Department of Electrical Engineering, Faculty of Engineering, Kafrelsheikh University, Kafr El-Shaikh 33511, Egypt (e-mail: manalemara@mail.ntua.gr).

Georgios D. Peppas is with Raycap S.A., 66100 Drama, Greece (e-mail: peppas@ece.upatras.gr).

Eleftheria C. Pyrgioti is with the Department of Electrical and Computer Engineering, University of Patras, 26504 Patra, Greece (e-mail: e.pyrgioti@ece.upatras.gr).

Demetrios D. Chronopoulos is with the Regional Centre of Advanced Technologies and Materials, Czech Advanced Technology and Research Institute (CATRIN), Palacký University Olomouc, 779 00 Olomouc, Czech Republic (e-mail: dimitrios.chronopoulos@upol.cz).

Aristides Bakandritsos is with the Regional Centre of Advanced Technologies and Materials, Czech Advanced Technology and Research Institute (CATRIN), Palacký University Olomouc, 779 00 Olomouc, Czech Republic, and also with the Nanotechnology Centre and the Centre of Energy and Environmental Technologies, VŠB–Technical University of Ostrava, 708 00 Ostrava, Czech Republic (e-mail: a.bakandritsos@upol.cz).

Sokratis N. Tegopoulos and Apostolos Kyritsis are with the School of Applied Mathematical and Physical Sciences, National Technical University of Athens, 15780 Athens, Greece (e-mail: stegopoulos@mail.ntua.gr; akyrits@central.ntua.gr).

Thomas E. Tsovilis is with the School of Electrical and Computer Engineering, Aristotle University of Thessaloniki, 54124 Thessaloniki, Greece (e-mail: tsovilis@auth.gr).

Aikaterini D. Polykrati and Ioannis F. Gonos are with the School of Electrical and Computer Engineering, National Technical University of Athens, 15780 Athens, Greece (e-mail: apolyk@mail.ntua.gr; igonos@cs.ntua.gr).

Color versions of one or more figures in this article are available at https://doi.org/10.1109/TDEI.2022.3163814.

Digital Object Identifier 10.1109/TDEI.2022.3163814

I. Introduction

HIGH-VOLTAGE (HV) equipment, such as transformers, capacitors, and circuit breakers, uses high amount of dielectric insulation oils for cooling and/or insulating [1]. Since 1887, mineral oils have been used due to their good performance, but their biodegradability problems are their main drawbacks [2]. To satisfy the environmental requirements, new natural insulating oils were proposed as an alternative to mineral oil. As these oil types come from natural sources, such as plants or seeds, they are fully biodegradable to overcome one of the main drawbacks of mineral oil [2]–[4]. In addition, the enhancement of the dielectric and thermal properties can be an asset to the dielectric withstand and insulation coordination design of large power transformers [1], [2].

To satisfy higher performance for the insulating oils, many researchers used different suspended nanoparticles in dielectric oils to form oil-based nanofluids. This new dielectric oil drew attention in the last few decades, so as to be used in different HV applications. The main target was to enhance dielectric properties [5]–[8] and/or enhance thermal conductivity properties [5], [9]–[11].

Different shapes of nanoparticles were used to enhance the thermal performance of oils, such as spherical, rod, nanotubes, nanosheets, and nanoplatelets. The used nanoparticles include different material types; nitrides [10], [12], carbon nanotubes [9], [13], oxides [14], diamonds [15], graphene [4], [13], [16], and hybrid [7], [17] have been used for thermal properties enhancement for different oils.

It is well known, based on recently published literature that graphene, especially in nanosheets, exhibits good performance in enhancing thermal conductivity properties [4], [13], [16]. Thus, this article uses a special type of graphene nanosheets, as described in Section II, to enhance the thermal properties of the natural ester oil. In addition, dielectric properties were studied based on dielectric relaxation spectroscopy (DRS) measurements. Also, the homogeneity of the prepared nanofluid was further examined by means of UV–visible absorbance spectroscopy.

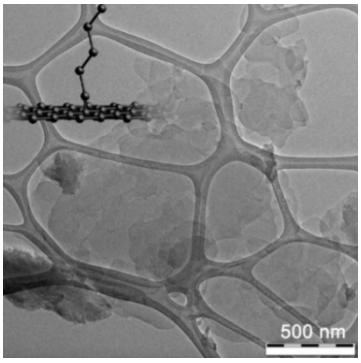

Fig. 1. TEM image of the pentyl-graphene sheets and respective model (inset).

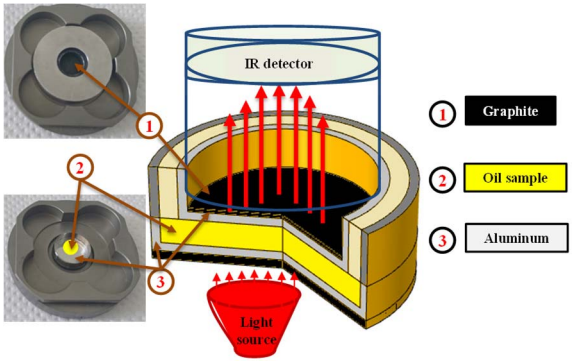

Fig. 2. LFA test cell.

II. Experimental Section

A. Materials Used

Pentyl-graphene derivative was prepared according to the literature [18]. 60 mg of exfoliated fluorographene, obtained by ultrasonic exfoliation of the commercial graphite fluoride, was suspended in 20 ml of dry tetrahydrofuran (THF) with the aid of sonication for 4 h. Afterward, pentyl-magnesium bromide (10 mmol) was added dropwise to the above suspension, and the reaction mixture was stirred under nitrogen for 5 h. In order to quench the unreacted Grignard reagent (pentyl-magnesium bromide), 30 ml of the saturated aqueous solution of NH_4Cl was added to the mixture. Subsequently, the organic layer, containing the graphene material, was collected and filtrated on a Whatman Nylon membrane filter (0.2 μm). In order to remove any magnesium salt residues, the material was resuspended in a solution of 5% HCl. Finally, pentyl-graphene was obtained after consecutive suspensions in water, ethanol, and dichloromethane (DCM) and separation by centrifugations. DCM is an organic solvent, among other commonly used for the dispersion of hydrophobic nanoparticles due to its low surface tension and medium polarity [19]. According to the previous detailed structural characterization, the pentyl chain is covalently linked to the graphene backbone, with a degree of functionalization calculated at about 8.5%, suggesting a high loading of aliphatic pentyl-groups, also explaining its excellent dispersibility in DCM [18]. TEM microscopy from a DCM dispersion showed that pentyl-graphene was composed of exfoliated few-layered graphene sheets with a lateral size smaller than ca. 1000 nm (see Fig. 1). The inset in the top left corner of Fig. 1 shows the structure of the pentyl-chain covalently attached to the graphene backbone.

B. Nanofluid Preparation

Natural ester oil (Envirotemp FR3) from Cargill was used as a matrix oil, prefiltered with a 30 μm filter paper (under vacuum with Buchner funnel) and poured through a Whatman[1] glass microfiber filters Multigrade GMF 150 (1 μm) in a glass filter holder assembly to remove any residual impurities in the dielectric liquid [20]. Filtering process includes prefiltering (30 μm) and filtering (1 μm) the dielectric liquid so as to avoid any misleading results due to any impurities [21]. Matrix oil was dehumidified accordingly by means of a rotary evaporator while heated in a water bath under 80 °C with a moisture content of 40 ppm, after the treatment.

The solution of pentyl-graphene nanosheets dispersed in DCM was accurately weighted (per concentration) and added to the matrix dielectric liquid at different concentrations. Thereafter, the nanofluid was mechanically agitated and left in an ultrasonic bath (BK-1200) for 30 min prior to each test sequence. The nanofluids' concentrations used in the study were 0%, 0.001%, 0.004%, 0.006%, 0.008%, 0.01%, and 0.012% w/w.

C. Thermal Conductivity

Based on Fourier's law of heat conduction in (1), the thermal conductivity (λ) was obtained from measuring thermal diffusivity (α) and specific heat values (c_p) [22]

$$\lambda = \alpha * c_p * \rho \tag{1}$$

where ρ is the density value (g/cm^3) for each sample that was kept constant; for FR3 at ambient temperature according to its datasheet, $\rho = 0.92$ g/cm^3.

D. Thermal Diffusivity

Based on the flash method, the thermal diffusivity (α) was measured by NETZSCH LFA 467 Hyper Flash apparatus using the specific cell for liquids. For the preparation of the test cell, a layer of graphite was used to coat its top and bottom, so as to help in the transmission of the radiation through the sample inside the LFA device, as shown in Fig. 2. Three light pulse shots of heat transmission were used to measure thermal diffusivity values at each temperature from 30 °C to 90 °C with a step of 10 °C. Thermal diffusivity was estimated by employing the half-time method via (2) [22]. The measured shots are analyzed on the basis of the three-layer model and fitting a Cowan pulse-correction model

$$\alpha = \frac{1.38 * L^2}{\pi^2 * t_{1/2}} \tag{2}$$

where L and $t_{1/2}$ are the sample thickness and the half time that is required to obtain the maximum temperature on the opposite side, respectively.

[1]Registered trademark.

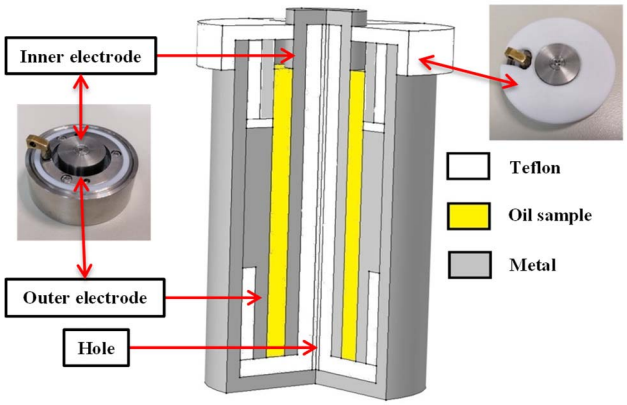

Fig. 3. DRS test cell.

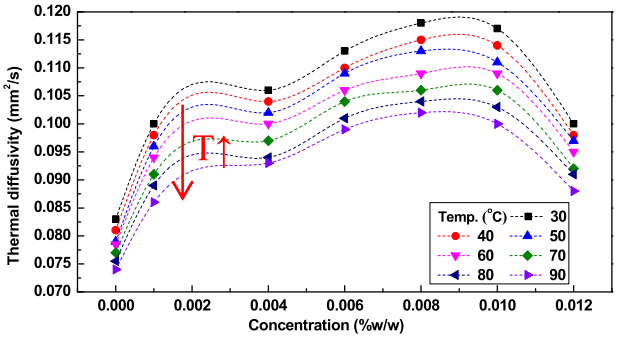

Fig. 4. Thermal diffusivity for nanofluid samples.

E. Specific Heat

The measurement of specific heat values was important to complete the investigation of the thermal properties of nanofluid samples with the aid of differential scanning calorimetry (DSC, TA Q200 instrument). The device was calibrated with indium for temperature and enthalpy and with sapphires for heat capacity. Each oil sample was sealed inside a Tzero Aluminum Hermetic pan. A fixed ramp rate (2 °C/min) was applied, starting from 10 °C up to 100 °C as a final temperature.

F. Dielectric Relaxation Spectroscopy

The relative permittivity and electrical conductivity were studied for nanofluid samples via Broadband dielectric spectroscopy (Novocontrol Alpha Analyzer and Quatro Cryosystem) for a range of frequencies (0.1 Hz–1 MHz). In dielectric susceptibility measurements, the real and imaginary parts of dielectric permittivity are measured simultaneously. The samples were studied through heating temperatures (20 °C–100 °C) and cooling temperatures (95 °C–25 °C) with a step of 10 °C. The actual and simulation models of the used test cell (BDS 1307 cylindrical liquid cell by Novocontrol) are shown in Fig. 3.

The relative permittivity (ε_r) has a complex form as shown in the following equation:

$$\varepsilon_r = \acute{\varepsilon}_r - j\,\acute{\acute{\varepsilon}}_r \tag{3}$$

where $\acute{\varepsilon}_r$ and $\acute{\acute{\varepsilon}}_r$ are real and imaginary parts of relative permittivity that refers to dielectric constant and dielectric losses contributed by the leakage current and dielectric polarization. Based on dielectric losses, the electrical conductivity (σ) can be obtained by the following equation:

$$\sigma = \omega \varepsilon_o \acute{\acute{\varepsilon}}_r \tag{4}$$

where ω and ε_o are the angular frequency and the vacuum permittivity, respectively [23].

G. UV–Visible Absorbance

Visible spectra were collected on an Analytik Jena SPECORD S600 spectrophotometer, in the form of solutions/dispersions in DMF. The measurements of light scattering of graphene sheets dispersed in the oil were performed with a ZetaSizer Nano series Nano-ZS (Malvern Instruments Ltd., Malvern, U.K.) equipped with a He−Ne laser beam at a wavelength of 633 nm and a fixed backscattering angle of 173°.

III. Results and Discussion

A. Thermal Diffusivity

The thermal diffusivity has been measured at different temperatures for the prepared samples following the procedure presented in Section II-D. For the recalculations step of thermal diffusivity values, the average specific heat values of the three measured times for the matrix oil and a constant value of density value were used. Fig. 4 shows the effect of nanofluid concentration and the applied temperature on the thermal diffusivity values. Any increment in the temperature results in decreasing the thermal diffusivity values for the matrix oil and nanofluid samples.

The thermal diffusivity of the nanofluids is mainly affected by the matrix oil (FR3), which is confirmed by the experimental results of the natural ester oil thermal diffusivity and thermal conductivity trend; the same trend is followed by the nanofluids as well [4].

The thermal diffusivity gradually increases up to the saturation limit of 0.008% w/w. Above the latter concentration (0.008% w/w), the enhancement decreases due to the agglomeration of part of nanoparticles that will be discussed and further supported by UV and DRS experimental results (see Sections III-D and III-E). Nevertheless, nanofluids with 0.01% w/w and 0.012% w/w nanoparticles concentration had higher enhancement of the thermal diffusivity with respect to the pure oil matrix (FR3) with values reaching up to 40.51% and 22.78% at 50 °C, respectively. The thermal diffusivity, from the trend line, has an expected maximum between 0.008% w/w and 0.010% w/w; still, the maximum measured thermal diffusivity was found at 0.008% w/w marginally higher than 0.010% w/w. The highest obtained enhancement of thermal diffusivity was 43.04% for the nanofluid concentration of 0.008% w/w at 50 °C. Based on (2), higher thermal diffusivity values translate into faster heat dissipation of the cooling medium. The latter thermal diffusivity enhancement may attribute to the fast heat dissipation and, thus, also temperature reduction within HV equipment [3].

TABLE I
SPECIFIC HEAT FOR VARIOUS TEMPERATURES FOR THE MATRIX OIL

Temperature (°C)	30	40	50	60	70	80	90
Average (J/g.k)	1.62	1.63	1.65	1.66	1.68	1.70	1.72
Standard deviation (%)	2.70	3.16	3.04	2.67	2.15	1.54	0.88

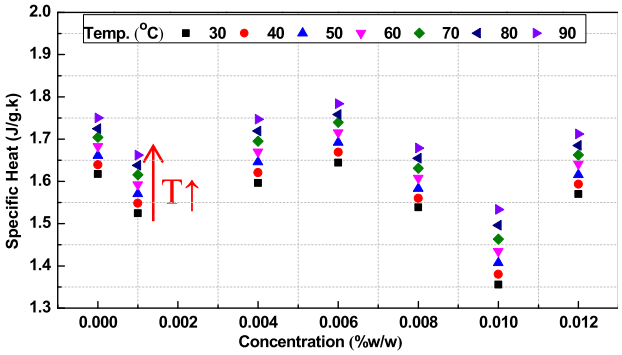

Fig. 5. Specific heat values for all samples.

B. Specific Heat

The specific heat of the matrix oil was measured three times per temperature. Due to the low standard deviation of the measurements, as shown in Table I, the specific heat of the nanofluids was measured once per temperature and per concentration.

Fig. 5 shows the specific heat values under the effect of changing temperature and different nanofluid concentrations. It demonstrates that the specific heat for any sample increases by increasing the temperature with approximately the same rate for the matrix oil and the nanofluid samples. As depicted in Fig. 5, the specific heat of the investigated nanofluids exhibited similar values compared with the matrix oil.

C. Thermal Conductivity

Fig. 6 shows the calculated thermal conductivity based on the measured thermal diffusivity and the specific heat values for each sample based on (1). It shows that thermal conductivity for all the samples is higher than its value of matrix oil, while it decreases by increasing temperature. The maximum value is acquired at 0.006% w/w; thereafter, a decreasing trend is recorded due to the decreased specific heat at 0.008% w/w (see Fig. 5), while, at 0.010% w/w and above, agglomeration mainly affects the decreased thermal diffusivity, specific heat and, as a result, the thermal conductivity.

D. Dielectric Relaxation Spectroscopy

1) Real Part of Relative Dielectric Permittivity: The real part of dielectric permittivity results was studied with respect to its dependence on frequency, temperature, and nanofluid concentration, as described in the following points based on Figs. 7 and 8 through the heating and cooling processes to study the possible hysteresis since the transformer operation includes both conditions under normal operation.

a) Frequency Dependence of $\acute{\varepsilon}_r$: For all samples, $\acute{\varepsilon}_r$ has a practically constant value (frequency-independent) at the kHz region and exhibits enhanced values at low frequencies (nearly less than 1 kHz). This polarization process is more pronounced

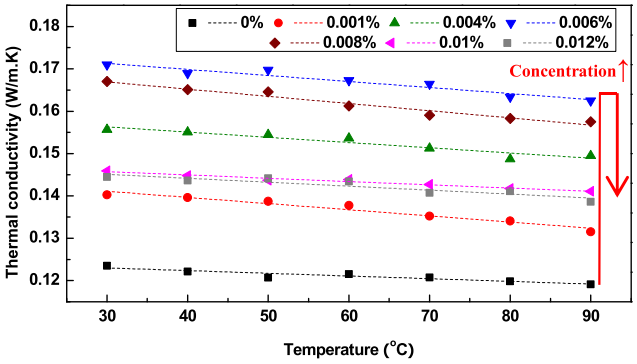

Fig. 6. Calculated thermal conductivity.

in the nanofluid samples. Taking into account that all samples exhibit long-range charge mobility (dc conductivity), this polarization process may be attributed to interfacial polarization of the Maxwell–Wagner–Sillars type and to electrode polarization [24]. The increase in ε' at the MHz region may be an artifact due to resonance effects in the measuring cell.

Of interest here is the origin of the high-frequency constant value of $\acute{\varepsilon}_r$ (electric polarizability). The value of around 3 at 40 °C for the matrix oil is marginally higher than the values of 2.1–2.4 usually recorded for mineral oils; still, these results are in line with the expected values for ester oil.

b) Temperature Dependence of $\acute{\varepsilon}_r$: For all nanofluid samples, such as in matrix oil, $\acute{\varepsilon}_r$ decreases with increasing temperature. Assuming that the main contribution in the polarizability arises from dipolar orientation processes, this temperature dependence of $\acute{\varepsilon}_r$ can be fully explained since dipole orientation polarizability scales with 1/T.

Measurements during heating and subsequent cooling reveal remarkable hysteresis effects. The values of $\acute{\varepsilon}_r$ for all the samples during cooling remain lower than those recorded during heating with the hysteresis effect being more pronounced at room temperature. This effect occurs also in the matrix oil, as shown in Fig. 8, probably more intense than in the nanofluid samples. Therefore, the interpretation of the effect shall be based, mainly, on the properties of the matrix. In the literature of liquids, and especially of insulating liquids, such hysteresis effects have already been described; however, their origin has not been fully explored yet. It can be outgassing of water, dissolution of gases, and aging effects at elevated temperatures [25].

c) Nanofluid Concentration Dependence of $\acute{\varepsilon}_r$: The dependence of $\acute{\varepsilon}_r$ on various concentrations of the inclusions is of interest, particularly for the low understudied frequencies. Fig. 9 shows the $\acute{\varepsilon}_r$ (f) curves obtained on all samples at $T = 40$ °C. It is obvious that the low-frequency polarization processes are more pronounced in the nanofluid samples becoming rather stronger by increasing graphene loading (a similar obtained trend with the dc conductivity of the nanofluid samples that will be described in Section III-D2c). The highest obtained enhancement in the dielectric constant was 6.18% at 0.008% w/w.

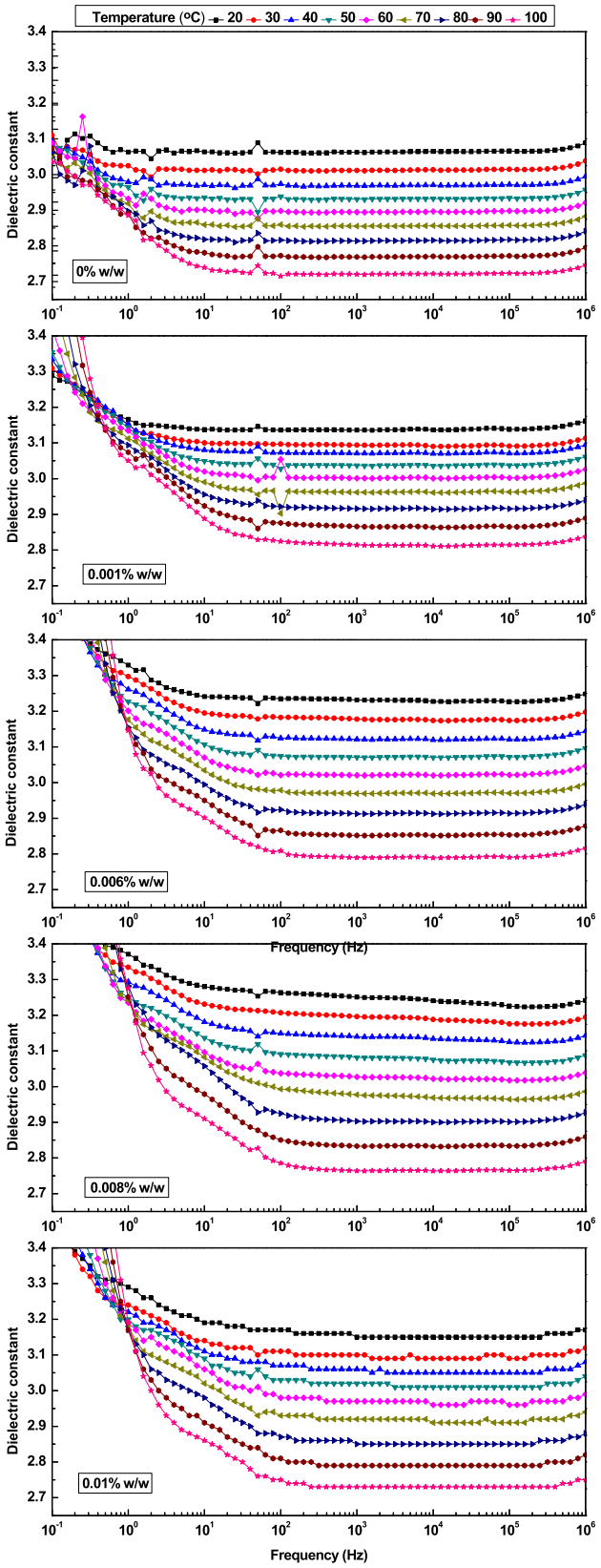

Fig. 7. Real part of the relative dielectric permittivity of all samples.

For the nanofluid sample with the high concentration (0.01% w/w), $\acute{\varepsilon}_r$ decreases, exhibiting, thus, a maximum at a lower concentration. This composition dependence is clearly shown in Fig. 14, and its result is similar to that obtained

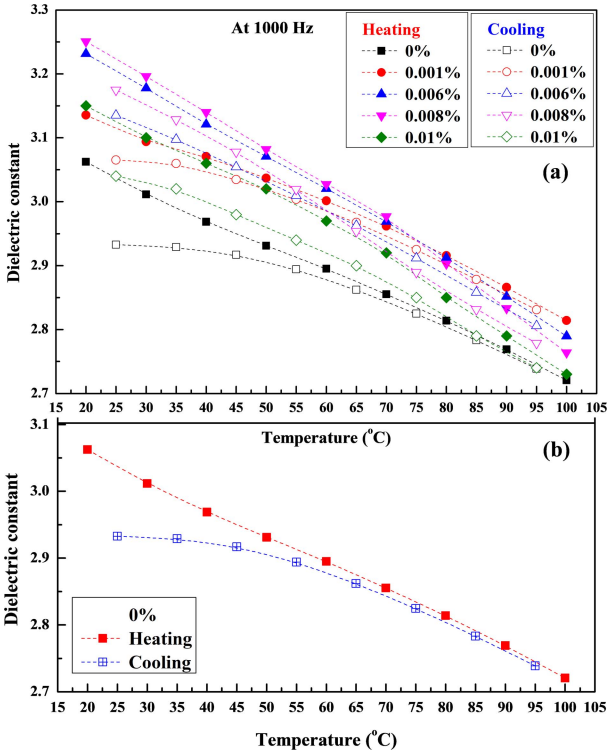

Fig. 8. Dielectric constant at *1* kHz through heating and cooling process for (a) all concentrations and (b) matrix oil.

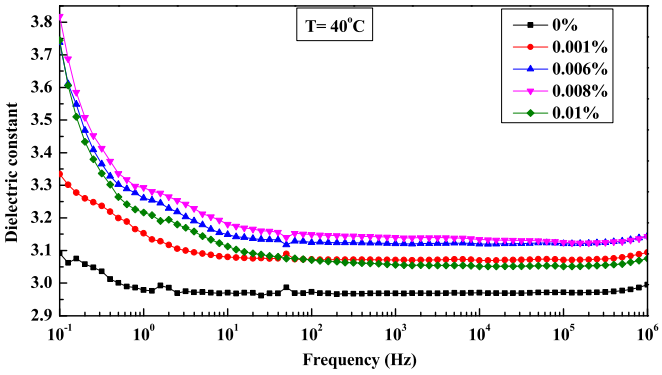

Fig. 9. Real part of the dielectric permittivity of all the studied samples.

for thermal diffusivity (see Fig. 4) and UV–visible absorbance (see Fig. 15) and may be associated with the agglomeration of nanosheets. The interpretation of this behavior is not a trivial task. In the literature, the polarizability of the oil-based nanofluid has been discussed using various concepts, such as effective medium theories, e.g., the Maxwell–Garnett formula and double-layer polarization processes in the nanoparticles or electrophoretic transactions, to name some of the models invoked [26]. The latter results also verify the accuracy of the measurements properly identifying the effect of the agglomeration through the DRS measurements having a good agreement with the thermal diffusivity results.

2) Electrical Conductivity (σ): As mentioned in (4), electrical conductivity is proportionally dependent on the imaginary part of relative permittivity; the results for the imaginary part for all the concentrations at 40 °C are presented in Fig. 10. The imaginary part demonstrates a

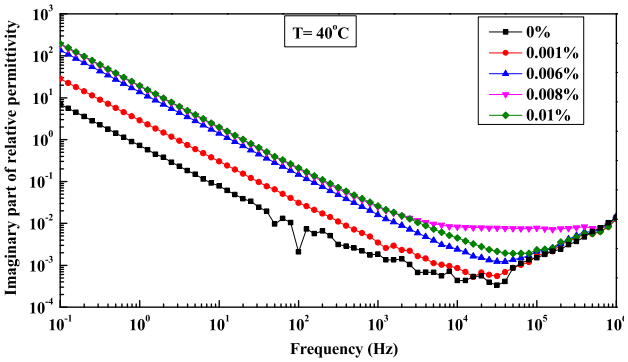

Fig. 10. Imaginary part of the relative permittivity of all the samples.

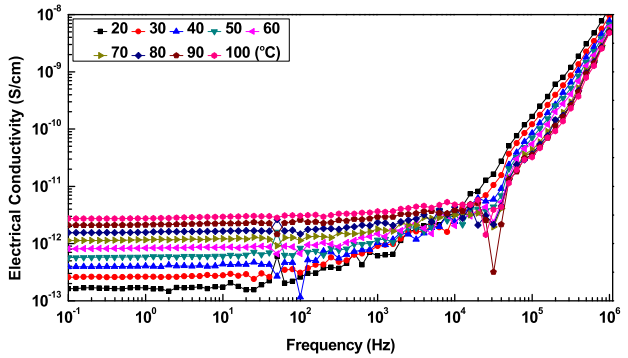

Fig. 11. Electrical conductivity (matrix oil).

decreasing trend, observed for all the samples up to 10–20 kHz. Saturation was observed on the nanofluid. Moreover, saturation was evidential for the nanofluid with 0.008% w/w, while the nanofluid with 0.010% w/w had a similar performance with 0.008%; the increased concentration does not differentiate due to the agglomeration effect (described in Sections III-A and III-E).

The electrical conductivity dependence on frequency, temperature, and nanofluid concentration was studied in the following paragraphs based on Figs. 11 and 12. Through the electric conductivity study, considering the matrix oil similar performance, the electrophoresis conductivity is mainly related to the viscosity of the base fluid. The total electric conductivity as per Shen *et al.*'s [27] electric conductivity model of nanofluids is dependent on the Maxwell conductivity and the dynamic electrical conductivity caused by the electrophoresis and Brownian motion of the nanoparticles.

a) Frequency Dependence of σ: As shown in all the previous figures, the electrical conductivity is frequency-independent in the low-frequency region indicating the activation of dc conductivity in the samples, though of very low value. At relatively high frequencies, the recorded charge motions are of shorter length scales, and the conductivity is higher and becomes frequency-dependent; a similar response was found by Dong *et al.* [28] for SiO_2-based nanofluids. The same trend of increasing electrical conductivity in the high-frequency region is identified for all the understudied dielectric liquids [29].

b) Temperature Dependence of σ: The data in Figs. 11 and 12 show that the dc conductivity increases with increasing temperature, indicating that the process is thermally activated. This temperature dependence holds

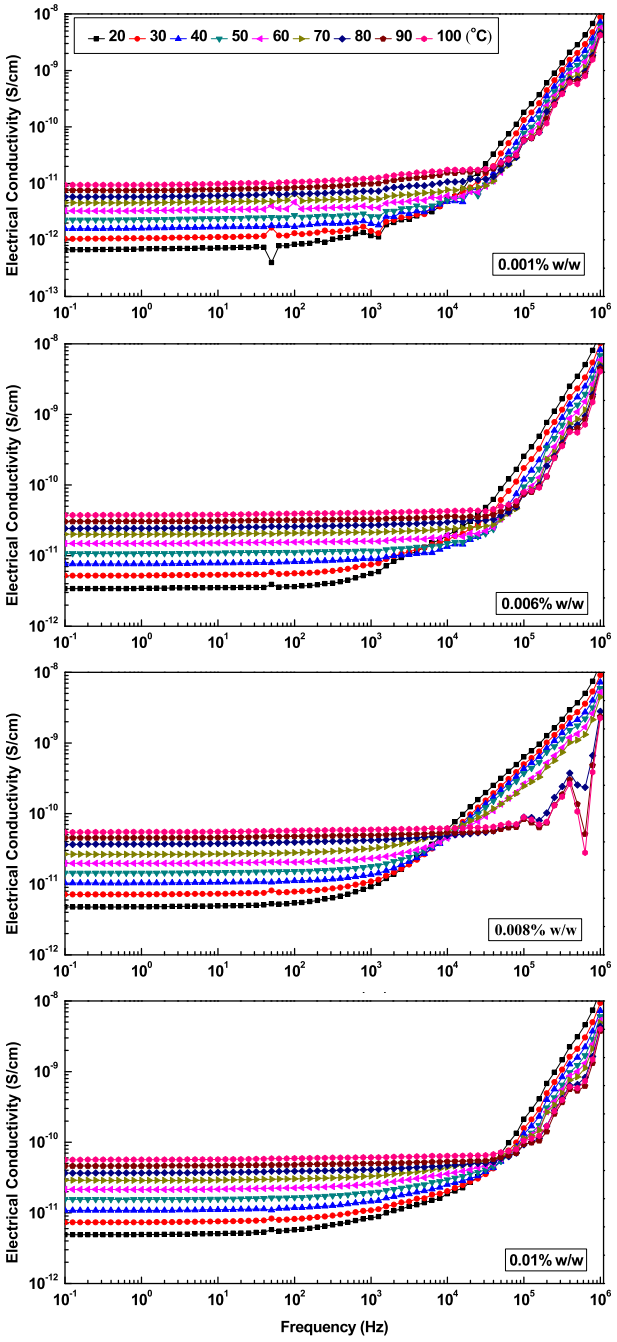

Fig. 12. Electrical conductivity of the prepared nanofluid samples.

for all the samples studied. Aiming at studying further the charge transport mechanism, the so-called activation map or the Arrhenius plot for the dc conductivity was constructed, as shown in Fig. 13.

In Fig. 13, the dc conductivity was plotted versus the reciprocal of temperature in a semilogarithmic plot so that the slope of each curve is directly related to the activation energy of the charge transport process. The data in Fig. 13 reveal that the conduction process does not change significantly in the oils of this work (matrix oil and nanofluid samples) since the activation energy, E_{act}, is similar in the matrix oil and the nanofluid samples ($E_{act} = 0.33$ eV). Interestingly, the values of σ_{dc} in the nanofluid samples at temperatures above 70 °C seem to deviate from the Arrhenius behavior at lower temperatures.

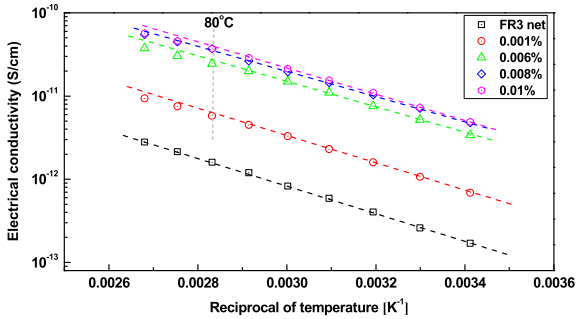

Fig. 13. Arrhenius diagram of the dc conductivity of all the studied samples.

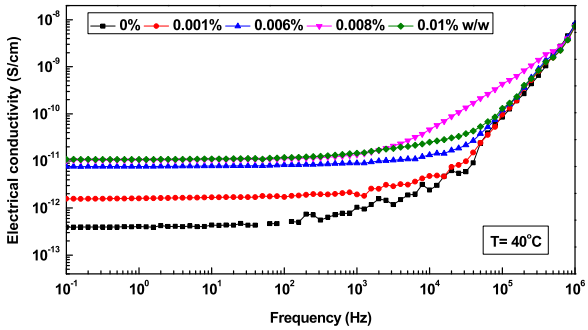

Fig. 14. Electrical conductivity of all the samples.

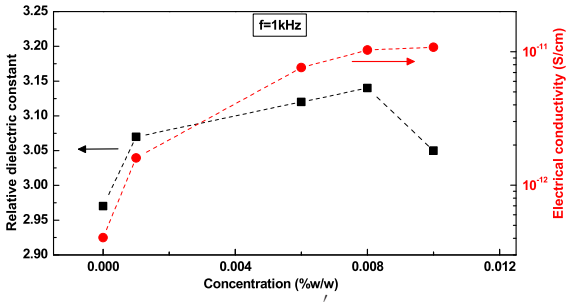

Fig. 15. Concentration dependence of $\acute{\varepsilon}_r$ (at 1 kHz) and dc conductivity, σ_{dc}, at 40 °C.

This finding may imply that the conduction process in the nanofluid samples changes slightly in this specific temperature range.

c) Nanofluid Concentration Dependence of σ: Fig. 14 shows electrical conductivity values based on the frequency range for all the samples at $T = 40$ °C. It is obvious that the dc electrical conductivity values increase with increasing nanofluid concentration, exhibiting saturation at the high concentrations, as described in Fig. 15. This conclusion is similar to that obtained for the thermal diffusivity (see Fig. 4) and UV–visible absorbance (see Fig. 16).

3) Nanofluid Concentration Dependence of $\acute{\varepsilon}_r$ and σ: Fig. 15 shows the dependence of the real part of relative dielectric permittivity and electrical conductivity on nanofluid concentration at 40 °C. It is clear that $\acute{\varepsilon}_r$ reaches a maximum value at around 0.008% w/w, while the dc conductivity increases constantly with increasing graphene concentration tending to saturation for higher concentration (>0.008% w/w).

E. UV–Visible Absorbance

The absorbance spectra of the oil-based nanofluid samples in Fig. 16 clearly showed the presence of a band at 330 nm

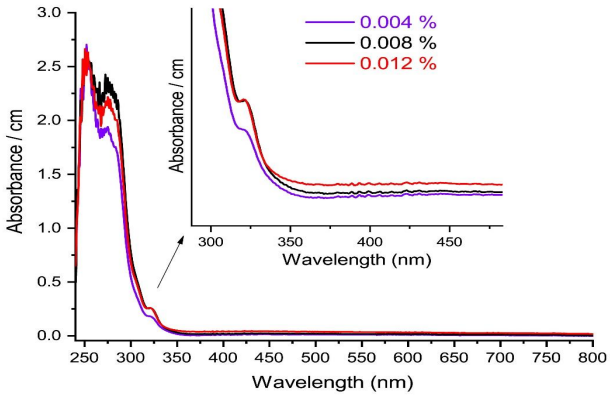

Fig. 16. UV–visible absorbance spectra of three mixtures of oil/pentyl-graphene at increasing concentrations in pentyl-graphene.

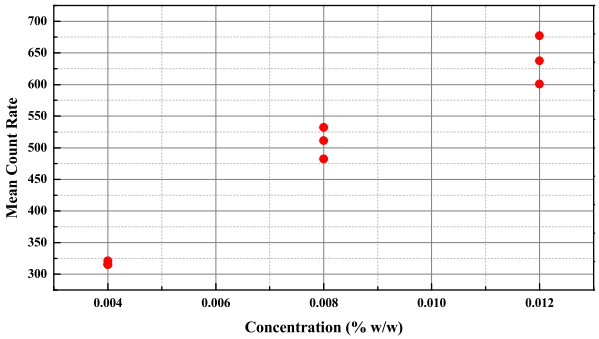

Fig. 17. Light scattering measurements of oil/pentyl-graphene mixtures at increasing concentrations ($n = 3$).

attributed to the graphene derivative (π–π^*) electronic transitions within long-ranged aromatic domains, which varied in intensity with changing nanofluid concentration [16]. The intensity increased going from 0.004% w/w to 0.008% w/w, but, upon further increase to 0.012% w/w, the intensity of the electronic absorption band remained the same. This clearly indicates the onset of agglomeration of the graphene sheets at the concentration of 0.012% w/w, inhibiting the electronic absorption at 330 nm. However, the scattering of light leading to the increased background absorption in the UV-Vis spectra consistently increased (linear part of the spectra in the inset of Fig. 16 for wavelengths >350 nm) unequivocally associated with the increased concentration in graphene sheets in the three samples. This was further confirmed from light scattering measurements (see Fig. 17), whereby the linearly increasing values of the intensity of the scattered light (i.e., the mean count rate) clearly designate the increasing concentration of nanoparticles (scatterers), while the agglomeration is identified from Fig. 16, wherein absorbance between 0.008% and 0.012% is marginally the same which clearly indicates an agglomeration effect.

IV. Conclusion

Pentyl-graphene nanosheets were suspended in FR3 natural ester dielectric oil, enhancing the thermal properties of the obtained nanofluid, while maintaining stable dielectric properties. Thermal diffusivity, specific heat, relative permittivity, and electrical conductivity studies in the range of 30 °C–90 °C showed a clear dependence of the final properties on graphene's concentration. In addition, UV–visible

absorbance was used to better explain the properties variation versus graphene's concentration. The important conclusions from this study are the following.

1) The optimum concentration that satisfied the best performance in thermal and dielectric properties was 0.008% w/w.
2) The highest obtained enhancement in thermal diffusivity was 43.04% at 50 °C.
3) The highest obtained enhancement in dielectric constant was 6.18% at 40 °C.

The used nanoparticles demonstrated high dispersibility in absence of agglomeration in the nanofluid state at the optimum concentration.

V. Acknowledgment

The authors highly acknowledge Kevin Rapp (Senior Scientist of Cargill) and Sabine Bowers from Cargill for the FR3 oil supply during this research.

References

[1] M. Rafiq, M. Shafique, A. Azam, and M. Ateeq, "The impacts of nanotechnology on the improvement of liquid insulation of transformers: Emerging trends and challenges," *J. Mol. Liquids*, vol. 302, Mar. 2020, Art. no. 112482.

[2] Z. Shen, F. Wang, Z. Wang, and J. Li, "A critical review of plant-based insulating fluids for transformer: 30-year development," *Renew. Sustain. Energy Rev.*, vol. 141, May 2021, Art. no. 110783.

[3] J. Jacob, P. Preetha, and T. K. Sindhu, "Stability analysis and characterization of natural ester nanofluids for transformers," *IEEE Trans. Dielectrics Electr. Insul.*, vol. 27, no. 5, pp. 1715–1723, Oct. 2020.

[4] M. M. Emara *et al.*, "Thermal and electrical conductivities for ester oil based graphene nana-sheets," in *Proc. IEEE Int. Conf. High Voltage Eng. Appl. (ICHVE)*, Sep. 2020, pp. 1–4.

[5] R. A. Farade *et al.*, "Investigation of the dielectric and thermal properties of non-edible cottonseed oil by infusing h-BN nanoparticles," *IEEE Access*, vol. 8, pp. 76204–76217, 2020.

[6] G. D. Peppas, V. P. Charalampakos, E. C. Pyrgioti, M. G. Danikas, A. Bakandritsos, and I. F. Gonos, "Statistical investigation of AC breakdown voltage of nanofluids compared with mineral and natural ester oil," *IET Sci. Meas. Technol.*, vol. 10, no. 6, pp. 644–652, Sep. 2016.

[7] P. Thomas *et al.*, "Synthetic ester oil based high permittivity $CaCu_3Ti_4O_{12}$ (CCTO) nanofluids an alternative insulating medium for power transformer," *IEEE Trans. Dielect. Elect. Insul.*, vol. 26, no. 1, pp. 314–321, Feb. 2019.

[8] A. J. Amalanathan, R. Sarathi, N. Harid, and H. Griffiths, "Investigation on flow electrification of ester-based TiO2 nanofluids," *IEEE Trans. Dielectrics Electr. Insul.*, vol. 27, no. 5, pp. 1492–1500, Oct. 2020.

[9] S. Daviran, A. Kasaeian, H. Tahmooressi, A. Rashidi, D. Wen, and O. Mahian, "Evaluation of clustering role versus Brownian motion effect on the heat conduction in nanofluids: A novel approach," *Int. J. Heat Mass Transf.*, vol. 108, pp. 822–829, May 2017.

[10] B. X. Du and X. L. Li, "Dielectric and thermal characteristics of vegetable oil filled with BN nanoparticles," *IEEE Trans. Dielectr. Electr. Insul.*, vol. 24, no. 2, pp. 956–963, Apr. 2017.

[11] A. Hameed *et al.*, "Experimental investigation on synthesis, characterization, stability, thermo-physical properties and rheological behavior of MWCNTs-kapok seed oil based nanofluid," *J. Mol. Liquids*, vol. 277, pp. 812–824, Mar. 2019.

[12] D. Liu, Y. Zhou, Y. Yang, L. Zhang, and F. Jin, "Characterization of high performance AIN nanoparticle-based transformer oil nanofluids," *IEEE Trans. Dielectr. Electr. Insul.*, vol. 23, no. 5, pp. 2757–2767, Oct. 2016.

[13] A. Naddaf and S. Z. Heris, "Experimental study on thermal conductivity and electrical conductivity of diesel oil-based nanofluids of graphene nanoplatelets and carbon nanotubes," *Int. Commun. Heat Mass Transf.*, vol. 95, pp. 116–122, Jul. 2018.

[14] D. C. Katpatal, A. B. Andhare, and P. M. Padole, "Viscosity behaviour and thermal conductivity prediction of CuO-blend oil based nano-blended lubricant," *Proc. Inst. Mech. Eng., J, J. Eng. Tribol.*, vol. 233, no. 8, pp. 1154–1168, 2018.

[15] G. Shukla and H. Aiyer, "Thermal conductivity enhancement of transformer oil using functionalized nanodiamonds," *IEEE Trans. Dielectr. Electr. Insul.*, vol. 22, no. 4, pp. 2185–2190, Aug. 2015.

[16] E. Rommozzi *et al.*, "Reduced graphene oxide/TiO_2 nanocomposite: From synthesis to characterization for efficient visible light photocatalytic applications," *Catalysts*, vol. 8, no. 12, p. 598, Dec. 2018.

[17] S. Aberoumand and A. Jafarimoghaddam, "Tungsten (III) oxide (WO_3)—Silver/transformer oil hybrid nanofluid: Preparation, stability, thermal conductivity and dielectric strength," *Alexandria Eng. J.*, vol. 57, no. 1, pp. 169–174, Mar. 2018.

[18] D. D. Chronopoulos *et al.*, "High-yield alkylation and arylation of graphene via Grignard reaction with fluorographene," *Chem. Mater.*, vol. 29, no. 3, pp. 926–930, Feb. 2017.

[19] P. Vineeth *et al.*, "Influence of organic solvents on nanoparticle formation and surfactants on release behaviour *in-vitro* using costunolide as model anticancer agent," *Int. J. Pharm Pharm Sci.*, vol. 6, no. 4, pp. 638–645, 2014.

[20] J. Zhang, J. Li, D. Huang, X. Zhang, S. Liang, and X. Li, "Influence of nonmetallic particles on the breakdown strength of vegetable insulating oil," in *Proc. IEEE Conf. Electr. Insul. Dielectr. Phenomena (CEIDP)*, Oct. 2015, pp. 609–612.

[21] X. Wang and Z. D. Wang, "Particle effect on breakdown voltage of mineral and ester based transformer oils," in *Proc. Annu. Rep. Conf. Electr. Insul. Dielectr. Phenomena*, Oct. 2008, pp. 598–602.

[22] P. A. Klonos, S. N. Tegopoulos, C. S. Koutsiara, E. Kontou, P. Pissis, and A. Kyritsis, "Effects of CNTs on thermal transitions, thermal diffusivity and electrical conductivity in nanocomposites: Comparison between an amorphous and a semicrystalline polymer matrix," *Soft Matter*, vol. 15, no. 8, pp. 1813–1824, 2019.

[23] M. M. Emara, D.-E.-A. Mansour, and A. M. Azmy, "Mitigating the impact of aging byproducts in transformer oil using TiO2 nanofillers," *IEEE Trans. Dielectr. Electr. Insul.*, vol. 24, no. 6, pp. 3471–3480, Dec. 2017.

[24] R. Richert, *Nonlinear Dielectric Spectroscopy*. Cham, Switzerland: Springer, 2018.

[25] A. Carey, *The Dielectric Constant of Lubrication Oils*. Knoxville, TN, USA: Computer Systems, Inc., 1998.

[26] J. Miao, M. Dong, M. Ren, X. Wu, L. Shen, and H. Wang, "Effect of nanoparticle polarization on relative permittivity of transformer oil-based nanofluids," *J. Appl. Phys.*, vol. 113, no. 20, May 2013, Art. no. 204103.

[27] L. P. Shen, H. B. Wang, M. Dong, Z. C. Ma, and H. B. Wang, "Solvothermal synthesis and electrical conductivity model for the zinc oxide-insulated oil nanofluid," *Phys. Lett. A*, vol. 376, no. 10, pp. 1053–1057, 2012.

[28] M. Dong, J. Dai, Y. Li, J. Xie, M. Ren, and Z. Dang, "Insight into the dielectric response of transformer oil-based nanofluids," *AIP Adv.*, vol. 7, no. 2, Feb. 2017, Art. no. 025307.

[29] F. Kremer and A. Schönhals, *Broadband Dielectric Spectroscopy*. Cham, Switzerland: Springer, 2002.

Manal M. Emara (Member, IEEE) was born in Kafr El-Shaikh, Egypt, in 1989. She received the B.Sc. degree in electrical power and machines engineering from Kafrelsheikh University, Kafr El-Shaikh, in 2011, the M.Sc. degree in electrical power and machines engineering from Tanta University, Tanta, Egypt, in 2016, and the Ph.D. degree from the School of Electrical and Computer Engineering, National Technical University of Athens (NTUA), Athens, Greece, in 2021.

Since 2012, she has been with the Electrical Engineering Department, Kafrelsheikh University, where she is currently an Assistant Professor. Her research interests are high-voltage engineering and nanodielectric materials.

Dr. Emara received the IEEE Caixin Sun and Stan Grzybowski Best Student Paper Award from IEEE International Conference on High Voltage Engineering and Application (ICHVE) 2020.

Georgios D. Peppas (Member, IEEE) was born in Rustenburg, South Africa, in 1987. He received the Diploma degree in electrical engineering and the Ph.D. degree from the Department of Electrical and Computer Engineering, University of Patras, Patra, Greece, in 2011 and 2016, respectively.

He is currently an R&D Manager of Raycap, Drama, Greece, leading innovation in surge protective devices, where he has been the Technical Manager of the High Current Laboratory since 2016. He is the author of four patents and more than 35 papers in major scientific journals and conference proceedings. His research interests include lightning and surge protection, and nanofluids for high-voltage applications.

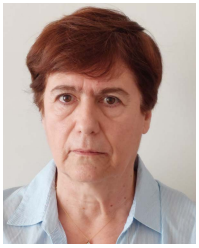

Eleftheria C. Pyrgioti (Member, IEEE) was born in Karditsa, Greece, in 1958. She received the Diploma degree in electrical engineering and the Ph.D. degree from the Electrical and Computer Engineering Department, University of Patras, Patras, Greece, in 1981 and 1991, respectively.

She is currently a Professor with the Electrical and Computer Engineering Department, University of Patras. Her research interests concern high-voltage systems, lightning protection, high-voltage insulation, dielectric liquids' distributed generation, and renewable energy.

Demetrios D. Chronopoulos was born in Kalamata, Greece, in 1979. He received the B.Sc. degree in chemistry from the Aristotle University of Thessaloniki (AUTh), Thessaloniki, Greece, in 2005, the M.Sc. degree in organic chemistry from the National and Kapodistrian University of Athens (NKUA), Athens, Greece, 2008, and the Ph.D. degree from the National Hellenic Research Foundation (NHRF), Athens, in 2015.

Since 2016, he has been a Scientific Researcher with the Regional Centre of Advanced Technologies and Materials (RCPTM), Palacký University Olomouc, Olomouc, Czech Republic. His research interests focus on the development of novel approaches for the covalent modification of carbon allotropes.

Aristides Bakandritsos was born in Larisa, Greece, in 1977. He received the B.Sc. degree in chemistry from the Aristotle University of Thessaloniki (A.U.Th), Thessaloniki, Greece, in 2001, and the Ph.D. degree in chemistry from the National Centre of Scientific Research "Demokritos," Athens, Greece, in 2006.

In 2012, he was elected at the Department of Materials Science, University of Patras, Patras, Greece, as a Lecturer and later as an Assistant Professor, until 2015–2016, when he joined the Regional Centre of Advanced Technologies and Materials (RCPTM), Palacký University Olomouc, Olomouc, Czech Republic. His research results have been published in 100 peer-reviewed journal articles. His research is focused on the synthesis and functionalization of carbon nanomaterials and hybrid (organic/inorganic) nanocolloids for energy storage, catalysis, and biomedical applications.

Sokratis N. Tegopoulos was born in Athens, Greece, in 1977. He received the B.Sc. degree in natural sciences from the Hellenic Open University, Patras, Greece, in 2016, and the M.Sc. degree in applied physics from the School of Applied Mathematical and Physical Sciences, National Technical University of Athens (NTUA), Athens, in 2018, where he is currently pursuing the Ph.D. degree.

Within the research activity of the Dielectrics Group, Department of Physics, School of Applied Mathematical and Physical Sciences, NTUA, he participates in research projects and assists in teaching undergraduate and postgraduate students. His main area of interest is the study of structure-properties relationship in (bio)polymer nanocomposite materials.

Apostolos Kyritsis was born in Berlin, Germany, in 1966. He received the Diploma degree in physics and the Ph.D. degree in materials science-physics from the University of Athens, Athens, Greece, in 1988 and 1995, respectively.

He is currently an Associate Professor with the National Technical University of Athens (NTUA), Athens. He has published more than 150 scientific papers in major international peer-reviewed scientific journals and five book chapters. He has more than 200 contributions to international conferences and more than 50 to national conferences. His scientific interests include dielectric, thermal, and vapor sorption studies in ionic crystals, ceramics, polymers, and complex polymeric systems, and structure–property relationships in polymers, biopolymers, nanocomposites, and hydration properties of inorganic and organic materials.

Thomas E. Tsovilis (Senior Member, IEEE) was born in Piraeus, Greece, in 1983. He received the M.Eng. and Ph.D. degrees in electrical and computer engineering from the Aristotle University of Thessaloniki (AUTh), Thessaloniki, Greece, in 2005 and 2010, respectively.

He was the Director of the High Current Labs, Raycap, Drama, Greece, and Ljubljana, Slovenia, from 2012 to 2018. In 2018, he joined AUTh, where he is currently an Assistant Professor. His research interest includes the broad area of high-voltage engineering with emphasis given to electrical discharges, lightning protection, and insulation coordination for power systems.

Aikaterini D. Polykrati was born in Athens, Greece, in 1966. She received the Diploma and Ph.D. degrees from the School of Electrical and Computer Engineering, National Technical University of Athens (NTUA), Athens, in 1990 and 2005, respectively.

She has been a Laboratory Educational Personnel of the High Voltage and Electrical Measurements Laboratory, Electrical and Computer Engineering School, NTUA, since 2001. Her research interests include high-voltage testing, electrical measurements, and electrical contacts.

Ioannis F. Gonos (Senior Member, IEEE) was born in Artemisio, Greece, in 1970. He received the Diploma degree in electrical engineering and the Ph.D. degree from the National Technical University of Athens (NTUA), Athens, Greece, in 1993 and 2002, respectively.

He is currently an Associate Professor with NTUA. He is the author of more than 200 papers in scientific journals and conferences proceedings. His research interests concern grounding systems, dielectric liquids, high voltages, measurements, and insulators.